AVO responses as modelled with a finite-difference program

Peter M. Manning* and Gary F. Margrave

ABSTRACT

The standard set of AVO interface properties is used to compare the predictions of a Zoeppritz ray trace program and a finite-difference modelling program. The resulting amplitude curves are found to take similar shapes, but differ in the position of important features.

INTRODUCTION

The typical types of AVO responses are based on the Geophysics paper by Rutherford and Williams (1989), who presented what they called three classes of responses from gas sands. These were called high-impedance contrast sands, near zero contrast sands, and low contrast sands. An additional class was later added by Castagna (1998), of a porous sand overlain by a high velocity unit, to get what is now almost a standard set of classes.

Work has continued on AVO responses of these classic types and others, with more generalized conditions and fewer restrictions. Included in this work are papers in this volume, for example Haase and Ursenbach (2004). These papers generally assume that the superposition of plane waves at the reflection interface is sufficient to characterize the reflected and transmitted amplitudes. We propose to inspect this intersection point with finite-difference modelling displayed as moving wavefronts. For the present paper, most of the material will be comparisons of the final amplitudes.

MODEL PARAMETERS

Table 1. The velocities (in m/sec) and densities (in g/cc) for the layer above the Zoeppritz interface (1) and below (2).

Class	AVO 1	AVO 2	AVO 3	AVO 4
$\alpha 1$	2000	2000	2000	2000
$\beta 1$	879.9	879.9	879.9	1000
$\rho 1$	2.4	2.4	2.4	2.4
$\alpha 2$	2933	2400	1964	1599
$\beta 2$	1882	1540	1260	654.3
$\rho 2$	2	2	2	2.456

The parameters used to model each AVO class are specified in Table 1. The interface with the impedance contrasts listed in Table 1 was placed at 740 metres, and an explosive P-wave source was initiated at a depth of 19 metres. Surface displacements were

measured at offsets from the source of 0 to 1900 metres. Recording was continued until at least some of the shear wave energy reached the surface.

The finite-difference models all used a spatial sample rate of 2.4 metres, and a time sample rate of .0005 seconds. Each model was initiated at the centre of a symmetric medium, of which only the right half is shown. The right boundary was absorbing, and the bottom boundary (at 1200 metres) was rigid. The initiating pulse was a 30 Hz Ricker wavelet.

MODEL RESULTS

A snapshot of the AVO class 1 wavefields at a time of 0.95 seconds is shown in Figure 1. The five short straight lines on the interface are the angles of the wavefronts (supposed by the Zoeppritz program) for the offset at their centre. The centre point here might be called the quintuple point.

The vertical displacement recorded at the surface of the model is shown in Figure 2. The reflected pressure-wave has a zero offset time of 780 milliseconds, and it can be seen to have a polarity reversal. The converted wave has a much steeper slope. It has zero amplitude at zero offset, but could be extended to zero offset at approximately 1230 milliseconds. It may be seen much more clearly in Figure 4.

The amplitude of the reflected pressure-wave is plotted in Figure 3. The theoretical amplitude from the Zoeppritz program is the smooth curve plotted in black. The amplitude from the finite-difference program is plotted in two colours: blue for positive amplitudes; and red for negative amplitudes. These amplitudes are the maximum and minimum for each trace within narrow windows (about 15 ms., unique to this polarity reversal case), the windows shifted by an appropriate normal moveout curve. The polarity reversal shows a switch from the blue to the red curve at about 1100 metres. The intersecting ground roll energy creates the high amplitude events at about 650 metres.

The horizontal displacement recorded at the surface is shown in Figure 4, and is the complement to Figure 2. The pressure wave has very low amplitude until longer offsets are reached, but the converted shear wave is much higher amplitude than on the vertical recording.

The amplitude of the converted shear wave is plotted in Figure 5. Amplitudes are obtained from the horizontal displacement record shown in Figure 4. There is no polarity reversal in this case (and in the other cases that follow) so the amplitudes are plotted differently from the pressure case. The normal moveout controlled windows are widened to about 50 milliseconds to contain at least one full cycle of the wavelet. The absolute values of the maxima and minima are then plotted to compare with the Zoeppritz program.

The amplitude of a pressure wave reflected from an AVO class 2 interface is shown in Figure 6. The method of obtaining the curves was the same as for the converted wave in Figure 5, except for the source of the input data. For this plot the vertical and horizontal amplitudes were combined to make a power trace, with a polarity taken from the vertical

trace. This method should give amplitudes closer to the Zoeppritz program results, but because the shear waves were sometimes contaminated by pressure energy on this record, the pure horizontal record was sometimes used. The ground roll at 600 metres is particularly strong on this plot.

Figures 7, 9, and 11 show the converted shear wave reflection amplitudes for the AVO cases of 2, 3, and 4 respectively. For cases 2 and 4, the power form of input data were used, while for case 3 the x-displacement data were used. The selection was made for the best signal to noise ratio, the noise in these cases being ground roll or other reflections.

Figures 8 and 10 show the reflected pressure waves for AVO cases 3 and 4 respectively. Both of these used the power form of input data.

DISCUSSION OF THE MODEL RESULTS

In Figure 1, comparison of the position and orientation of the modelling wavefronts with those assumed for Zoeppritz calculations shows one of the limitations of the Zoeppritz method. In general, if the velocities in the lower medium are significantly higher than the upper medium, as the lower wavefront becomes more perpendicular to the interface it will tend to outpace the quintuple point. The wavefronts will tend to heal, but take the wrong angles. Eventually they will lose contact above and below the interface, and tend to disperse the wavefronts. Note that this can happen before the critical point.

The finite-difference modelling and the Zoeppritz programs show similar trends in most cases. For AVO case 1, the converted wave responses are almost identical, and the pressure wave responses shows similar polarity reversals, although not at quite the same places. The other AVO cases show that the trends of the modelling and the Zoeppritz results are similar. In conditions where the zero offset reflectivity is zero (for case 2 and all the converted waves), the two types of curves may be matched quite closely.

There are some general observations that may be made about the amplitude plots. Sharp features (at critical angles) are smoothed through with the finite-difference versions. The high points are often shifted between the two versions, but the causes are uncertain.

CONCLUSIONS

Finite-difference modelling has confirmed that Zoeppritz programs may make reasonable estimates of the amplitude variations with offset of the classic gas sand interfaces. However, the results differ in the details, and may be related to unrealistic assumptions at the quintuple point.

REFERENCES

Castagna, J.P., Swan, H.W., and Foster, D.J., 1998, Framework for AVO gradient and intercept interpretation: Geophysics, **63**, 948-956.

Haase, A. B. and Ursenbach, C. P., 2004, Spherical wave AVO modelling in elastic isotropic media: CREWES research report, v. **16**.

Rutherford, S.R., and Williams, R.H., 1989, Amplitude-versus-offset variations in gas sands: Geophysics, **54**, 680-688.

FIGURES

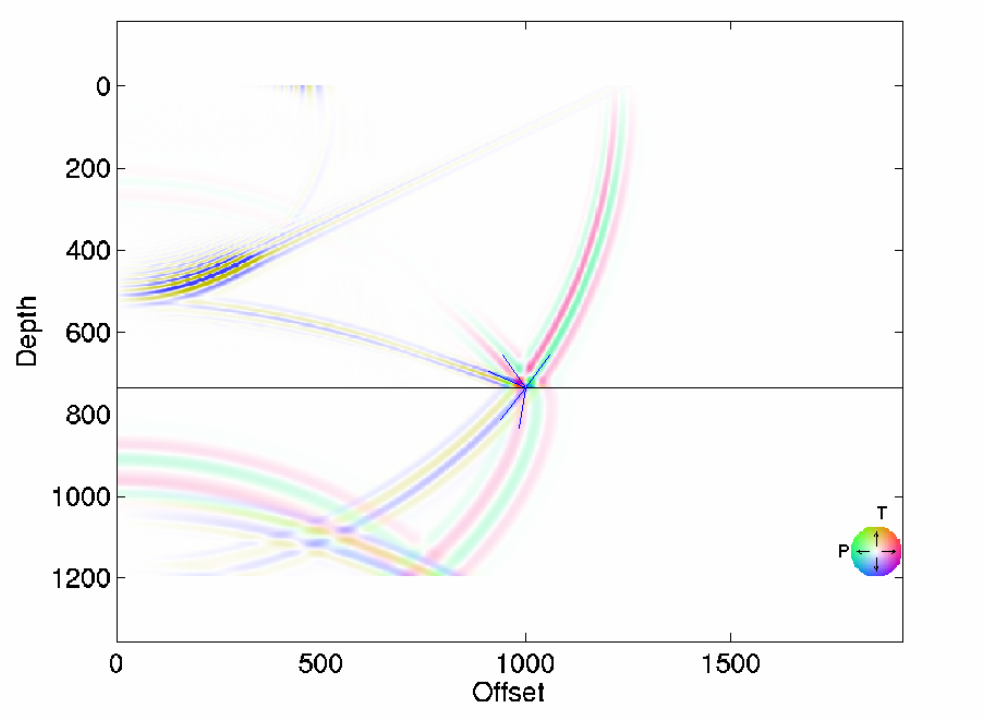

FIG. 1. A snapshot of the AVO class 1 wavefield at a time of 0.95 seconds. Straight lines indicate wavefront tangents used as input to the Zoeppritz equations at this offset.

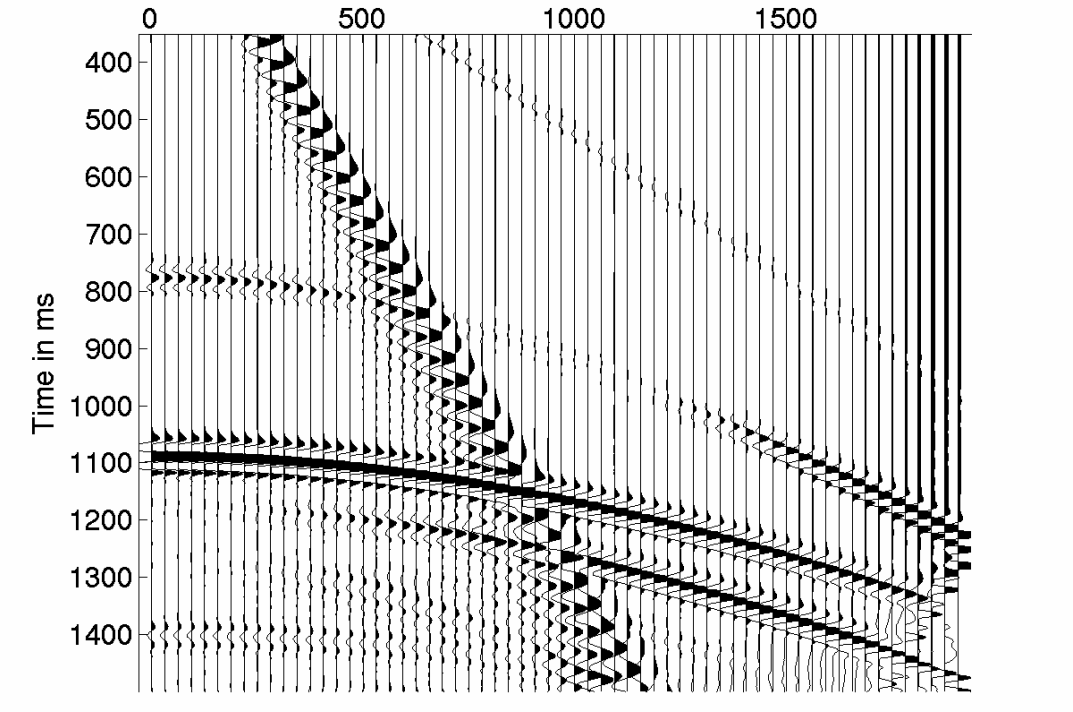

FIG. 2. AVO class 1 seismic section, vertical component. Pressure wave reflection at zero offset appears at time 780 ms.

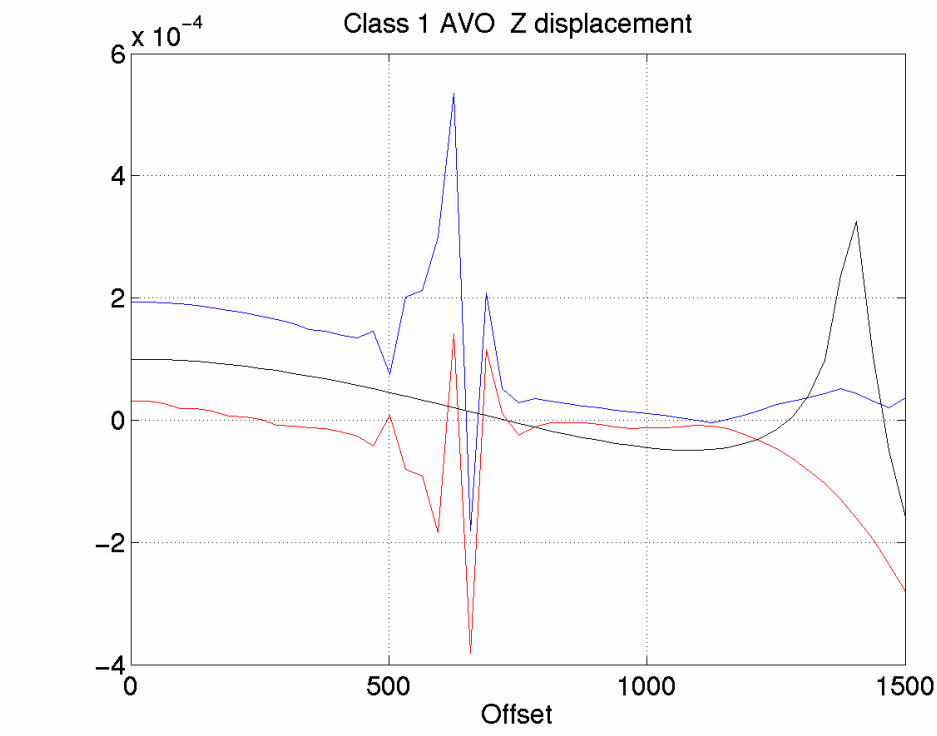

FIG. 3. Model amplitudes along the pressure reflection: positive blue; negative red. The smooth Zoeppritz curve is black. Note the ground roll interference at 600 – 700 metres.

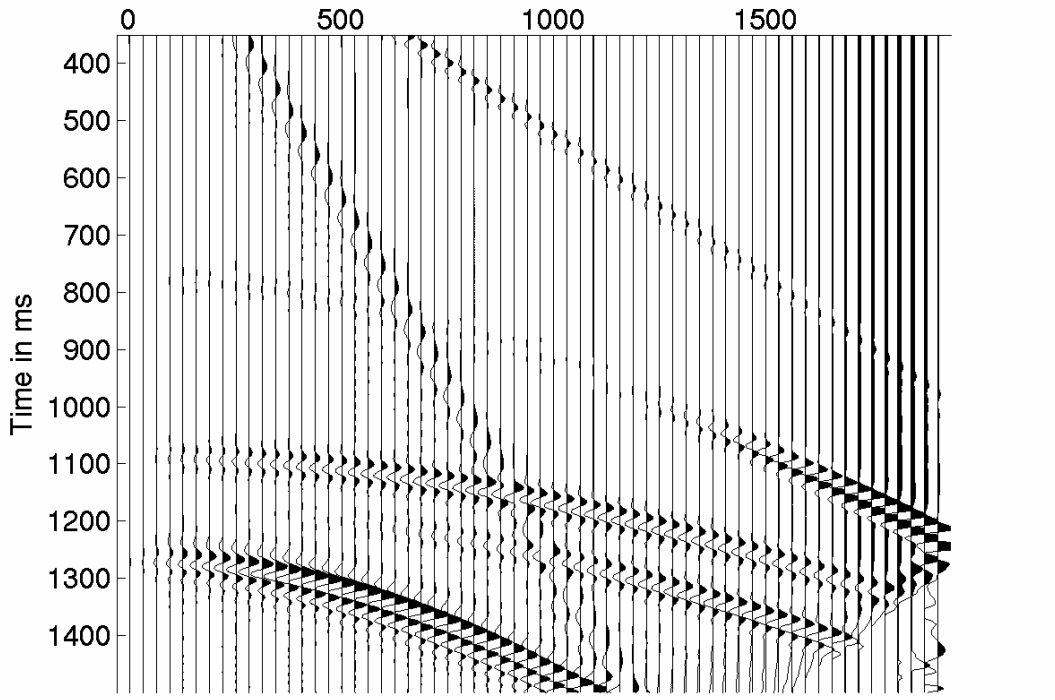

FIG. 4. AVO class 1 seismic section, horizontal component. Shear wave reflection at zero offset projects to about 1270 ms.

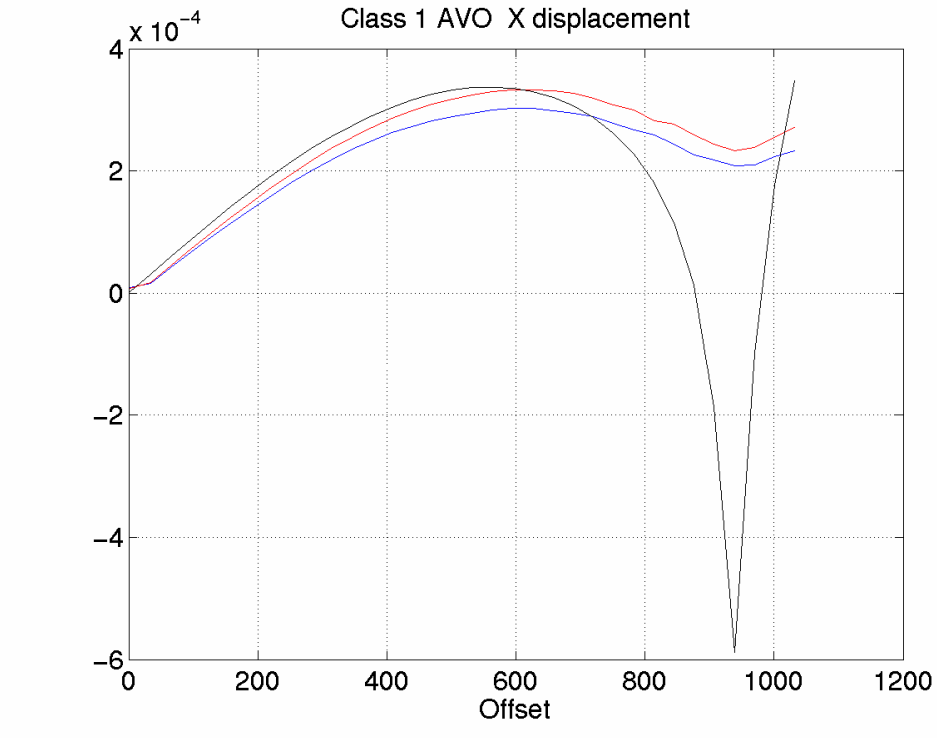

FIG. 5. Model amplitudes along the shear reflection, plotted positive. Peaks are plotted blue, troughs red. The Zoeppritz curve is black.

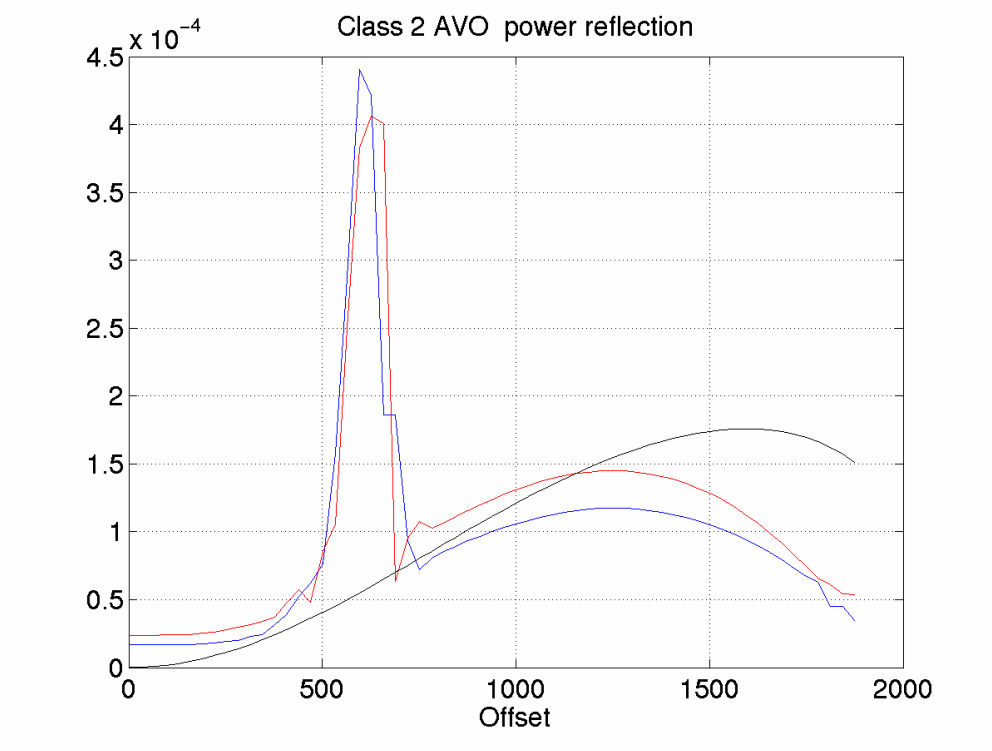

FIG. 6. Amplitudes along the pressure reflection of the class 2 model. The high amplitude points are caused by ground roll.

FIG. 7. Amplitudes along the converted reflection of the class 2 model. The smooth black trace results from the Zoeppritz calculations.

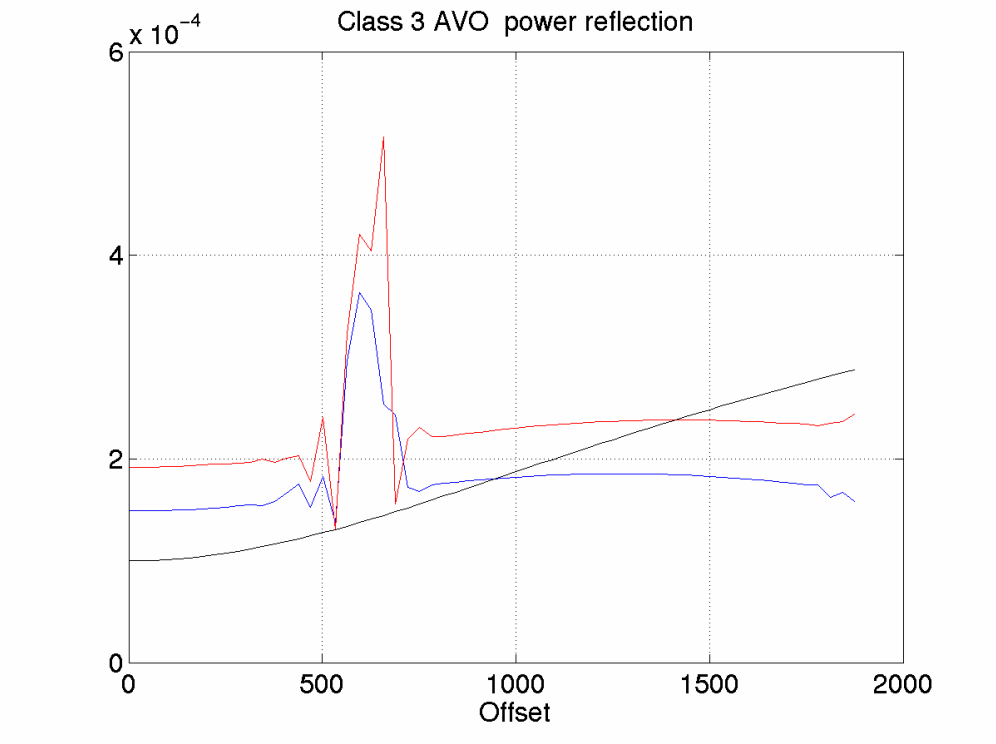

FIG. 8. Amplitudes along the pressure reflection of the class 3 AVO model. The high amplitude spikes are caused by ground roll.

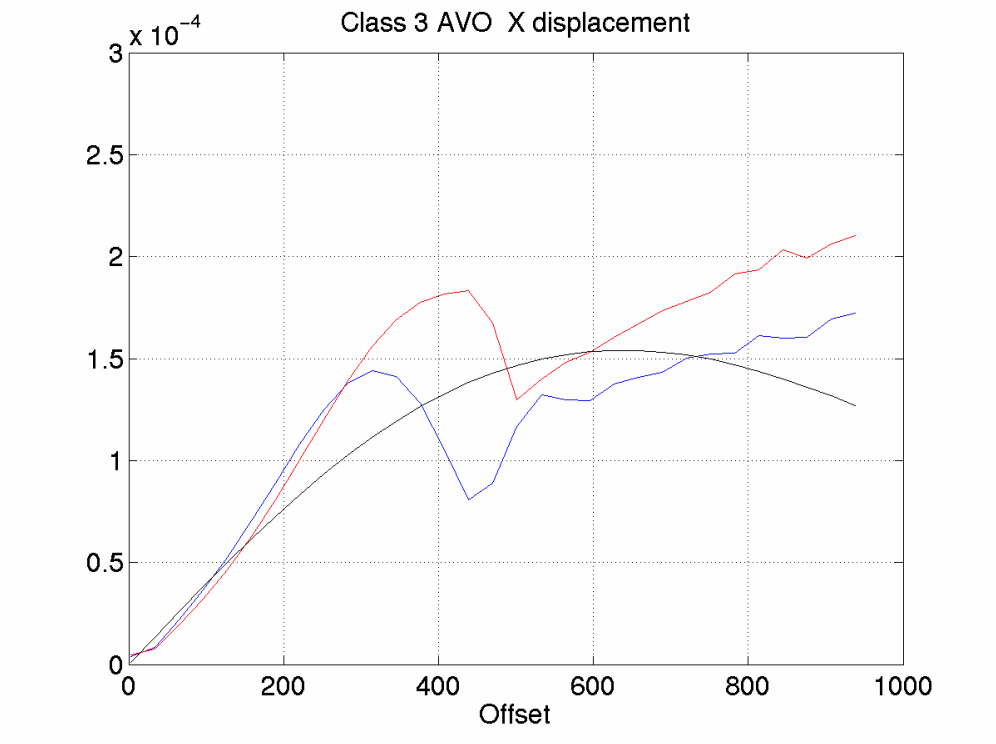

FIG. 9. Amplitudes along the converted reflection of the class 3 model. Some of the nearer traces show interference from another reflection.

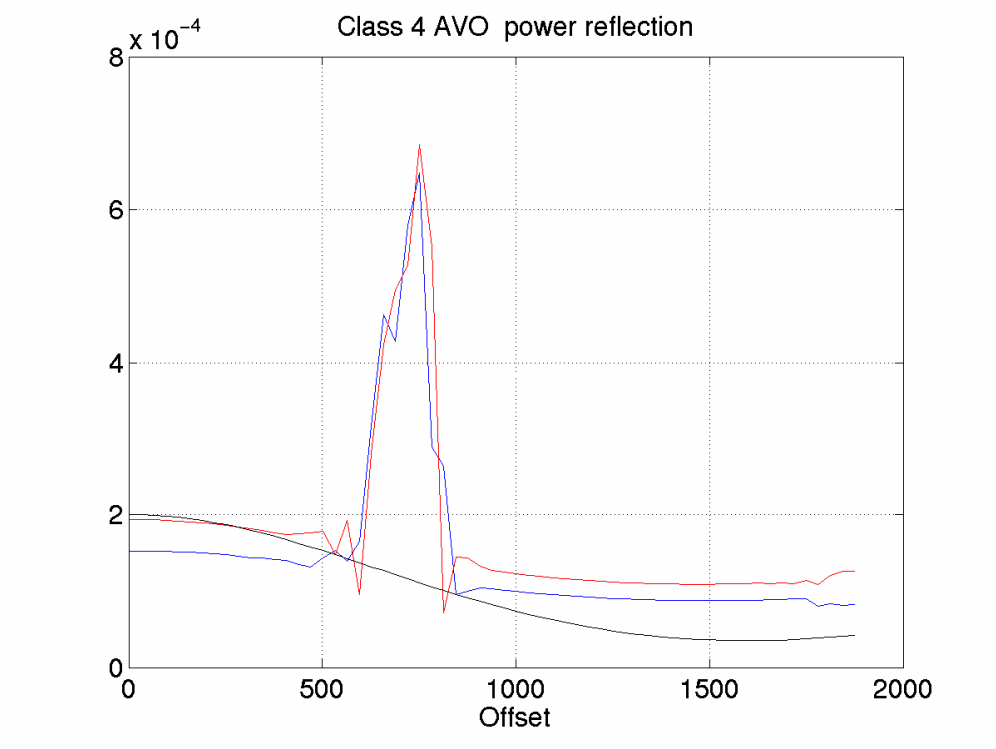

FIG. 10. Amplitudes along the pressure reflection of the class 4 model. The interfering energy is ground roll.

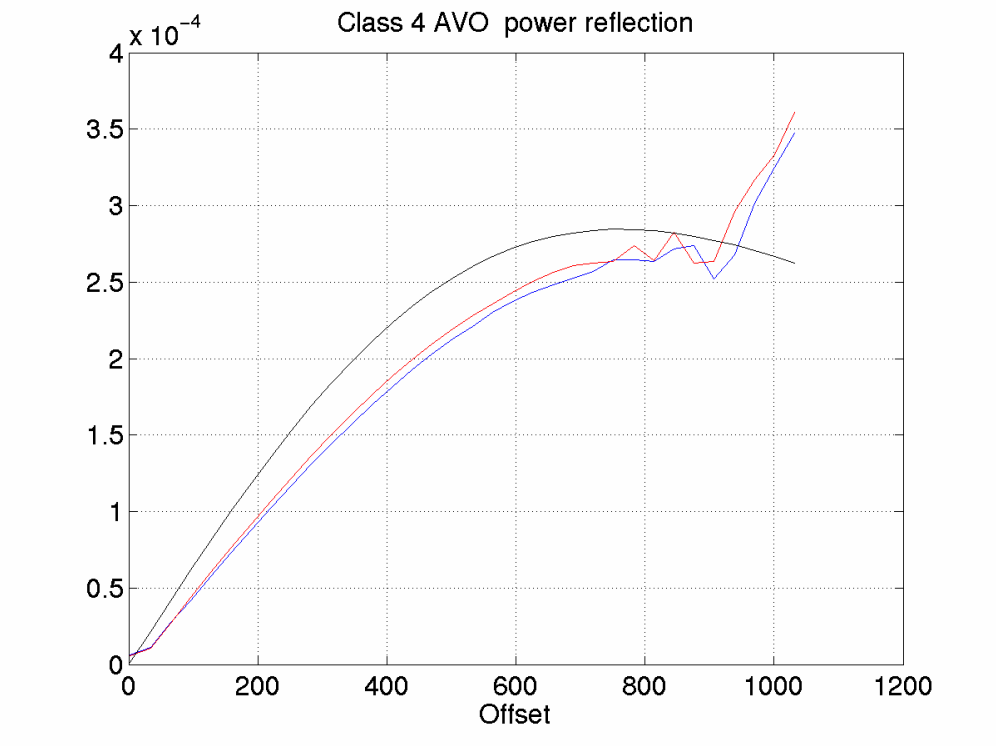

FIG. 11. Amplitudes along the converted reflection of the class 4 model. The end amplitudes are distorted by an intersection with another reflector.